AJNR

Anterior Spinal Artery and Artery of Adamkiewicz Detected by Using Multi-Detector Row CT

Kohsuke Kudo, Satoshi Terae, Takeshi Asano, Masaki Oka, Kenshi Kaneko, Satoshi Ushikoshi and Kazuo Miyasaka

Anterior Spinal Artery and Artery of Adamkiewicz Detected by Using Multi-Detector Row CT

Kohsuke Kudo, Satoshi Terae, Takeshi Asano, Masaki Oka,
Kenshi Kaneko, Satoshi Ushikoshi, and Kazuo Miyasaka

BACKGROUND AND PURPOSE: Our purpose was to evaluate the visualization of the artery of Adamkiewicz (AKA) and the anterior spinal artery (ASA) by using multi-detector row CT. Preoperative detection of the AKA and ASA is important for prevention of ischemic complications of thoracoabdominal aortic surgery.

METHODS: Data from contrast-enhanced CT of the abdomen of 19 consecutive patients with known or suspected liver disease were evaluated. The scanning range was set from the level of the diaphragm to the lower edge of the liver. After bolus injection of contrast material (100 mL of iohexol, 350 mgI/mL, 5 mL/s), arterial phase scans were obtained by using a four-channel multi-detector row CT scanner. The scanning parameters included a detector row configuration of 4 × 2 mm, a pitch of 5:1, a gantry rotation speed of 0.5 s, 120 kVp, and 150 mAs. Arterial phase coronal multiplanar reconstruction scans obtained parallel to the spinal cord were evaluated by two neuroradiologists. The detectability of ASA and AKA was analyzed.

RESULTS: The AKA was visualized on the scans of 13 of 19 patients (68%). The segmental level of AKA origin ranged from T10 to L2. The AKA originated from the left side in nine patients (69%) and the right side in four patients (31%). The ASA was visualized on the scans of all patients (100%). For 16 of the 19 patients, the ASA was detected in its full length from the cranial edge of the scan range. However, the ascending branch of the ASA distal to the junction of the AKA was not detected for the remaining three patients.

CONCLUSION: The AKA and ASA can be visualized by using multi-detector row CT with the use of IV administered contrast material. Multi-detector row CT could be a useful tool in the evaluation of spinal vascular structures.

Ischemic complication of the spinal cord after surgery of the thoracoabdominal aorta is a rare but serious event. The anterior two thirds of the spinal cord receive blood supply from the anterior spinal artery (ASA), which extends along the full length of the spinal cord (1). The ASA may be narrow at the thoracolumbar area and receives blood supply from the largest anterior radiculomedullary artery, called the *artery of Adamkiewicz* (AKA). The ASA and AKA play an important role in preventing spinal cord ischemia at the thoracolumbar area.

The causative factors for spinal cord ischemia after surgery of the thoracoabdominal aorta include systemic hypotension, prolonged aortic clamping, embolization, and interruption of internal iliac artery circulation (2). Although interruption of the AKA is not the sole cause of spinal cord ischemia (3), there have been reports of the importance of reattachment of the segmental arteries related to the AKA (4–6).

The AKA usually arises from the ninth intercostal artery to the second lumbar artery (1, 7). Although selective spinal arteriography is required to show the accurate level of AKA origin (6), a recently developed less invasive method of MR angiography could be used to detect AKA. It has been reported that the successful detection rate of AKA by MR angiography is 69% (8, 9).

CT angiography is another less invasive method with which to visualize small vessels. It has higher spatial resolution than does MR angiography, especially if a multi-detector row system is used. To our knowledge, there are few reports on visualization of intradural vessels by using contrast-enhanced CT angiography. The purpose of this study was to assess the visualization of ASA and AKA by using multi-detector row CT.

Methods

Participants

Nineteen consecutive patients with known or suspected liver disease underwent contrast-enhanced CT of the abdomen as a

TABLE 1: List of Patients and Results

Patient No.	Age (yr)	Sex	Background	Scanning Range		Range of ASA Detected		Level of AKA Origin
				Upper Limit	Lower Limit	Upper Limit	Lower Limit	
1	65	F	Chronic hepatitis	T8	L2	T10–T11	L1–L2	Right T11
2	52	F	Liver tumor	T8–T9	L2–L3	U	L1–L2	Left T10
3	54	M	Post-liver transplantation (donor)	T9	L2–L3	U	T12–L1	Left T10
4	76	M	HCC	T9	L2–L3	T10–T11	T12–L1	Left T11
5	71	M	HCC	T9	L2–L3	U	T12–L1	N.D.
6	57	F	Echinococcosis	T9	L2	U	L1–L2	N.D.
7	55	F	Liver cirrhosis	T9–T10	L3–L4	U	L	Left T10
8	51	M	HCC	T9–T10	L3	U	T12–L1	Right T11
9	73	M	HCC	T9–T10	L2–L3	U	L1–L2	N.D.
10	60	M	HCC	T9–T10	L2	U	T11–T12	Left T10
11	32	M	Post-liver transplantation (recipient)	T10	L3–L4	U	L12–L1	Right T11
12	51	M	Liver hemangioma	T10	L3–L4	U	L2–L3	N.D.
13	52	M	HCC	T10	L3	U	L	Left L1
14	56	M	HCC	T10	L2–L3	U	L	Right T12
15	48	F	Post-liver transplantation (recipient)	T10–T11	L4–L5	T11–T12	L1–L2	Left L2
16	68	M	Autoimmune hepatitis	T10–T11	L3	U	T12–L1	Left T11
17	25	M	Post-liver transplantation (recipient)	T11	L4	U	T12–L1	N.D.
18	64	M	HCC	T11	L3	U	T12–L1	Left L1
19	58	M	Liver cirrhosis	T11	L3	U	T12–L1	N.D.

Note.—ASA indicates anterior spinal artery; AKA, artery of Adamkiewicz; F, female; M, male; HCC, hepatocellular carcinoma; U, upper limit of scanning range; L, lower limit of scanning range; N.D., not detected.

routine part of liver investigation. The age of the patients ranged from 25 to 73 years (mean, 56.2 years). Fourteen male and five female patients were included. Among the 19 patients, 12 had liver cirrhosis or chronic hepatitis, with or without hepatocellular carcinoma; three had other types of liver tumor or tumorous lesions; and four had undergone liver transplantation. All patients were confirmed to have no aortic disease and no neurologic symptoms.

Scanning Protocol

All scans were obtained on a four-channel multi-detector row CT scanner (Aquilion; Toshiba Medical Systems, Tokyo, Japan). A 19- or 20-gauge catheter was inserted into a superficial vein at the antecubital fossa, forearm, or dorsum of the hand. One hundred milliliters of iohexol (350 mg/mL iodine) was injected at a rate of 5 mL/s.

The scanning range was set from the level of the diaphragm to the lower edge of the liver. An automatic bolus tracking technique monitoring aortic attenuation was used to obtain arterial dominant phase scans. Portal venous phase and delayed phase scans were also acquired to evaluate liver disease, although only the arterial phase scans were used in this study. Technical parameters included a detector row configuration of 4×2 mm, a pitch of 5:1, a gantry rotation speed of 0.5 s, 120 kVp, and 150 mAs.

Data Processing and Scan Evaluation

After data acquisition, axial arterial phase scans were reconstructed with a field of view of 20 cm and a section interval of 0.4 mm to render isotropic voxel data. Oblique-coronal multiplanar reconstruction scans along the long axis of the spinal cord were created with a section thickness of 1.2 mm and a section overlap of 50%.

The multiplanar reconstruction scans were displayed on the scanning workstation. Identification of the ASA and AKA on the multiplanar reconstruction scans was performed by two neuroradiologists (K.K., S.T.) who were in consensus. A vessel placed on the anterior midsagittal surface of the spinal cord was diagnosed as the ASA. The AKA was identified as the vessel that ascended

toward the anterior midsagittal surface of the spinal cord from the intervertebral foramen and joined the ASA via a characteristic hairpin configuration. The range of the ASA and the segmental level of the AKA origin were recorded.

Results

The results are summarized in the Table. The actual scanning ranges were different among the patients, because the scan was aimed to include the whole liver. The upper limit ranged from T8 to T11, depending on the level of the diaphragm, and the lower limit ranged from L2 to L4–L5, depending on the size of the liver.

The AKA was shown on the scans of 13 (68%) of 19 patients. The segment level of the AKA origin ranged from T10 to L2. The AKA originated from the left side in nine patients (69%) and from the right side in four patients (31%).

The ASA was visualized on the scans of all the patients. On the scans of three of the 19 patients, the AKA and the caudal portion of ASA distal to the junction of AKA were shown, but the cranial portion of the ASA was not detected. On the scans of 16 of the 19 patients, the ASA was detected in its full length from the cranial edge of the scanning range. On the scans of 10 of the 16 patients, the AKA and both cranial and caudal portions of the ASA distal to the junction of AKA were detected (Figs 1–3). On the scans of six of the 16 patients, only the ASA was visualized and the AKA was not detected (Fig 4).

Discussion

The AKA usually arises from the level of the ninth intercostal artery to the second lumbar artery (1). Be-
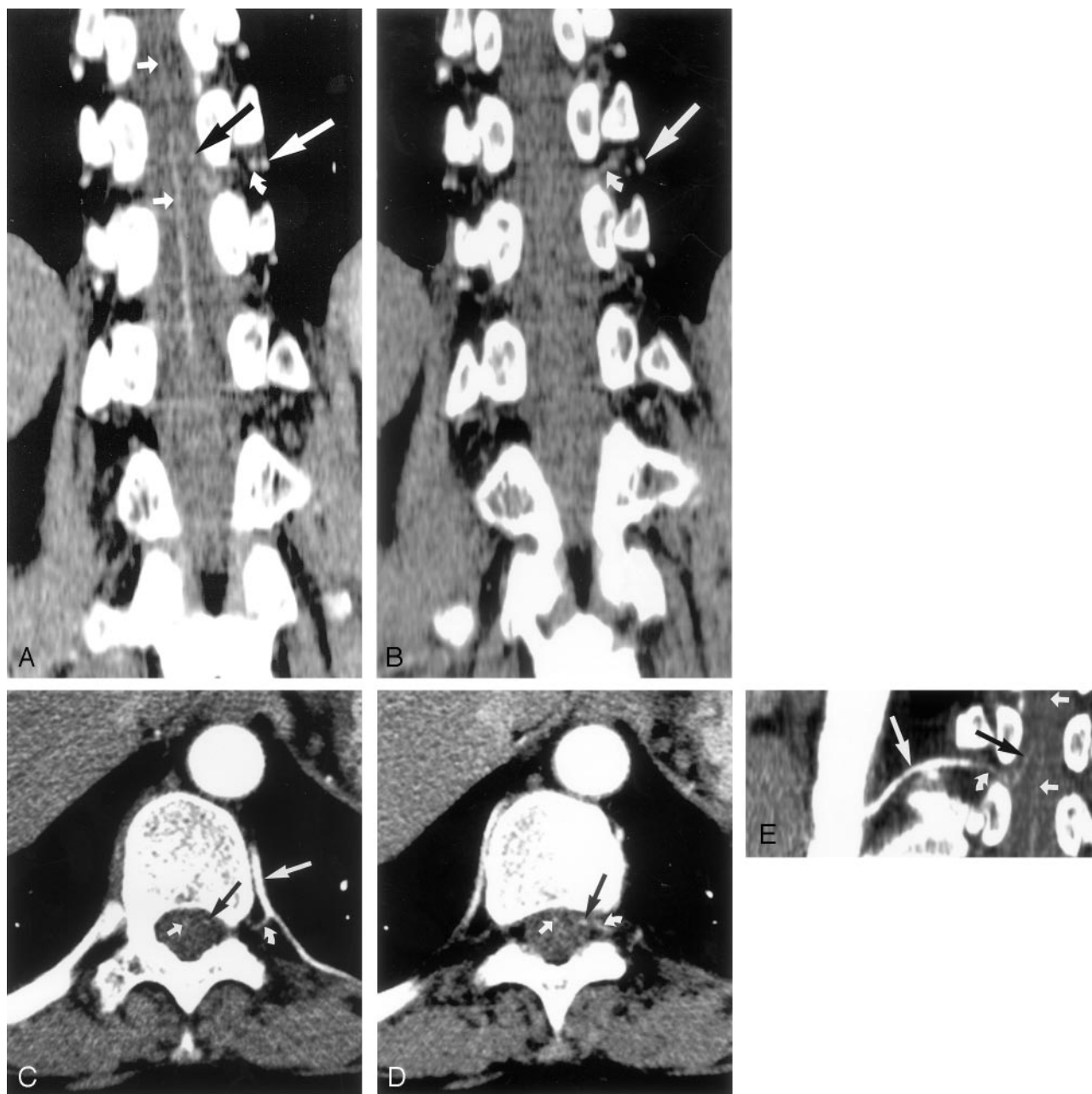
FIG 1.   CT scans obtained from patient 2, a 52-year-old woman.

A, Coronal multiplanar reconstruction scan shows the ASA along the anterior midsagittal surface of the spinal cord (*small white arrows*). The large radiculomedullary artery (*black arrow*), which is defined as the AKA, arises from the left T10 level and joins the ASA. Both the ascending and descending branches of the ASA distal to the junction with the AKA are seen, but the ascending branch is narrower than the descending branch. The spinal branch (*curved white arrow*) arises from the left 10th intercostal artery (*large white arrow*).

B, On the dorsal section of the coronal view, the continuity of the radiculomedullary artery and intercostal artery (*large white arrow*) via the spinal branch (*curved white arrow*) is confirmed.

C and *D*, Axial scans show the ASA (*small white arrows*) and AKA (*black arrows*) in the dural sac. The continuity of the intercostal artery (*large white arrow*), spinal branch (*curved white arrows*), and radiculomedullary artery (*black arrows*) is also seen.

E, Curved multiplanar reconstruction scan allows the visualization of the continuity of the intercostal artery (*large white arrow*), spinal branch (*curved white arrow*), radiculomedullary artery (*black arrow*), and ASA (*small white arrows*) on a single section. The change of caliber of these vessels is also seen.

cause the scanning data used in this study were those of routine abdominal CT aimed for the evaluation of liver disease, the scanning range was planned to cover the liver. Considering that it is not desirable to administer extra doses of irradiation, the scanning range was not extended to cover the whole area of possible AKA origin. In this study, the lower limit of the scanning range was at or below the L2 level in all patients, which is the level that is adequate to cover the lower origin of the AKA. However, the upper limit of the scanning range varied from the T8 to T11 level, and the AKA could have been located cranial to the scanning range in

FIG 2.   CT scans obtained in patient 3, a 54-year-old man.

A and *B*, Coronal scans show ASA (*small white arrow*) and AKA (*black arrows*). Thorough inspection reveals that the top of the hairpin curve is visualized at the upper edge of the scan. The continuity of the 10th intercostal artery (*large white arrow*), spinal branch (*curved white arrow*), and radiculomedullary artery (*black arrows*) is obscure because of close attachment of these vessels to the bone as a result of narrow intervertebral foramen.
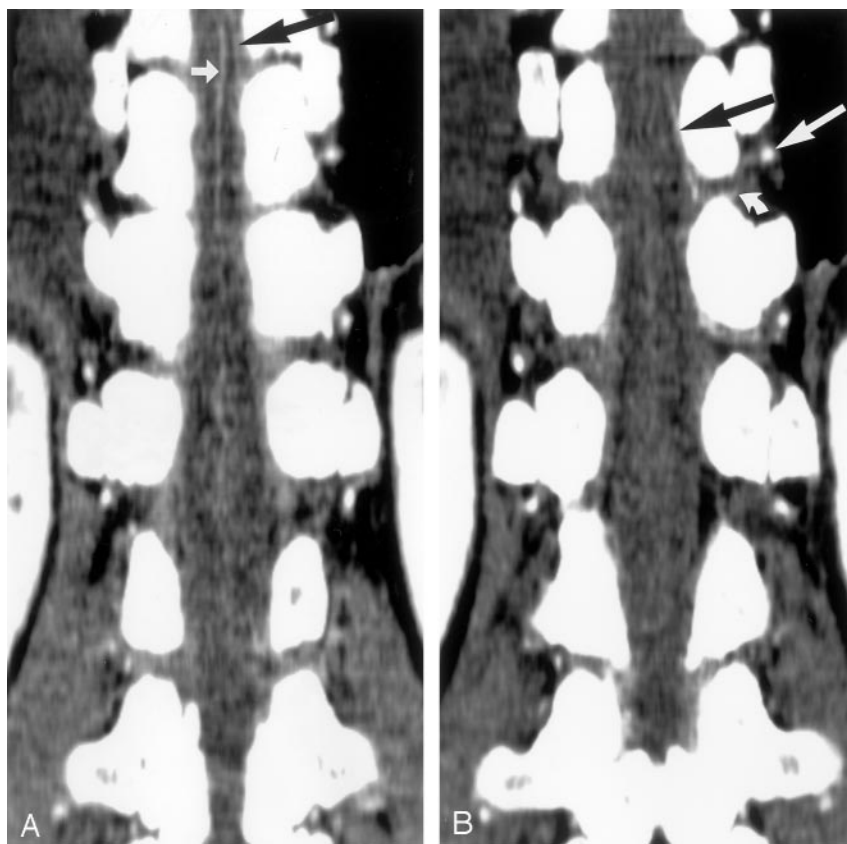
patients for whom AKA could not be detected. The inadequacy of the upper limit of the scanning range was the limitation of this study.

The detection ratio of AKA was 68% by using multi-detector row CT. It is comparable with the MR angiography results reported by Yamada et al (8, 9), with which the detection ratio of the AKA was 69%. Possible reasons for failure of visualization of the
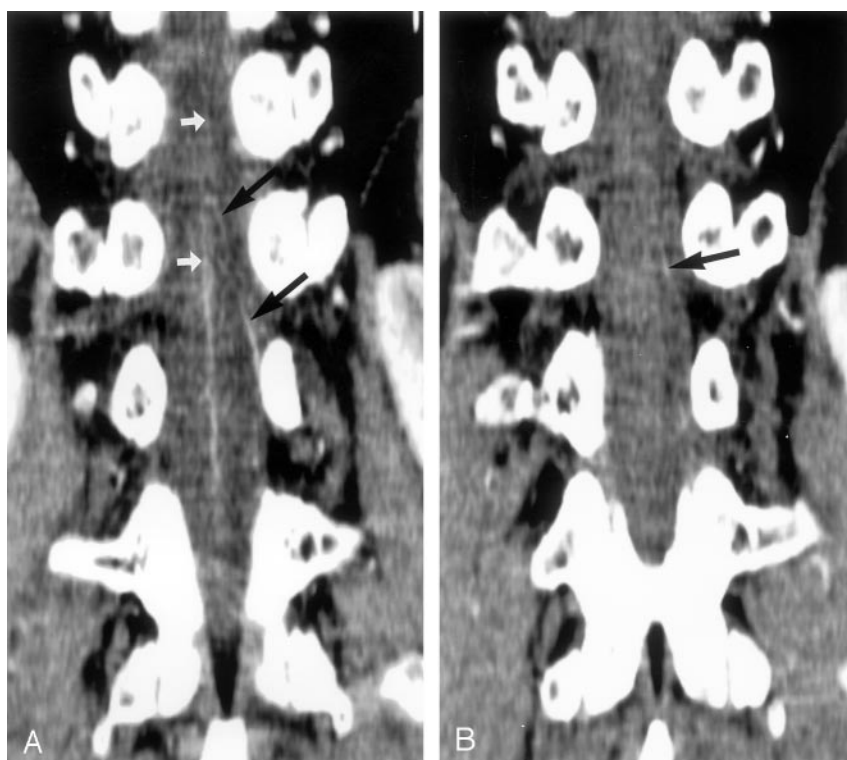
FIG 3.   CT scans obtained in patient 13, a 52-year-old man.

A, Coronal multiplanar reconstruction scan shows the radiculomedullary artery (*black arrows*) arising from the left L1 level and joining the ASA (*small white arrows*). Both the ascending and descending branches of the ASA are seen.

B, Because the radiculomedullary artery (*black arrow*) is slightly tortuous, the continuity of the vessel is confirmed on the section dorsal to that shown in *A*.
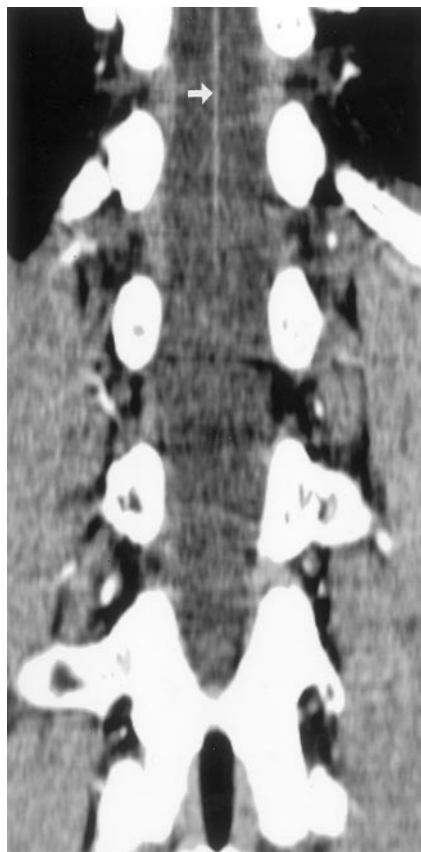
FIG 4. CT scan obtained in patient 17, a 25-year-old male patient. Coronal view multiplanar reconstruction scan shows the ASA (*small white arrow*) as visualized from the top of the scanning range. The radiculomedullary artery is not detected. The upper level of the scanning range is T11 level for this patient. The AKA is expected to arise from a more cranial level.

AKA in this study include inadequacy of the scanning range as discussed above, insufficient spatial resolution, and contrast-to-noise ratio. The diameters of the ASA and AKA are almost the same and are reported to be 0.5 to 0.8 mm at the thoracolumbar region (7). Because the ASA was detected for all patients, we think that the spatial resolution and contrast-to-noise ratio were sufficient for the visualization of the AKA. In this study, the segment level of the AKA origin ranged from T10 to L2 and the left side origin was 69%. Although the scanning range was limited, these results were in agreement with those of previous reports, including anatomic (1, 7) and MR angiography results (8, 9). For six patients for whom the AKA was not detected, the upper limit of the scanning range

varied from T9 to T11. For these patients, the ASA was visualized from the upper edge of the scanning range; it is thus possible that the AKA was located cranial to the scanning range. Therefore, if the scanning range had been adequate to cover the AKA origin, the detectability of the AKA would have been increased.

Although the descending branch of the ASA distal to the junction was shown on the scans of all the patients, the ascending branch of the ASA distal to the junction of the AKA was not shown on the scans of three patients. Because the ascending branch is almost always narrower than the descending branch, we speculate that for these patients, the spatial resolution was not sufficient for detecting the ascending branch, which has a smaller caliber.

Conclusion

The AKA and descending branch of the ASA can be detected by using multi-detector row CT if they are within the scanning range. CT angiography may be helpful in the evaluation of spinal cord circulation before and after aortic surgery and in the evaluation of spinal cord vascular diseases.

References

1. Tveten L. **Spinal cord vascularity: III. the spinal cord arteries in man.** *Acta Radiol Diagn (Stockh)* 1976;17:257–273
2. Rosenthal D. **Spinal cord ischemia after abdominal aortic operation: is it preventable?** *J Vasc Surg* 1999;30:391–397
3. Griepp RB, Ergin MA, Galla JD, et al. **Looking for the artery of Adamkiewicz: a quest to minimize paraplegia after operations for aneurysms of the descending thoracic and thoracoabdominal aorta.** *J Thorac Cardiovasc Surg* 1996;112:1202–1215
4. Safi HJ, Miller CC III, Carr C, Iliopoulos DC, Dorsay DA, Baldwin JC. **Importance of intercostal artery reattachment during thoracoabdominal aortic aneurysm repair.** *J Vasc Surg* 1998;27:58–68
5. Wan IY, Angelini GD, Bryan AJ, Ryder I, Underwood MJ. **Prevention of spinal cord ischaemia during descending thoracic and thoracoabdominal aortic surgery.** *Eur J Cardiothorac Surg* 2001;19:203–213
6. Heinemann MK, Brassel F, Herzog T, Dresler C, Becker H, Borst HG. **The role of spinal angiography in operations on the thoracic aorta: myth or reality?** *Ann Thorac Surg* 1998;65:346–351
7. Thron AK. *Vascular Anatomy of the Spinal Cord: Neuroradiological Investigations and Clinical Syndromes.* New York: Spinger-Verlag; 1988:3–65
8. Yamada N, Okita Y, Minatoya K, et al. **Preoperative demonstration of the Adamkiewicz artery by magnetic resonance angiography in patients with descending or thoracoabdominal aortic aneurysms.** *Eur J Cardiothorac Surg* 2000;18:104–111
9. Yamada N, Takamiya M, Kuribayashi S, Okita Y, Minatoya K, Tanaka R. **MRA of the Adamkiewicz artery: a preoperative study for thoracic aortic aneurysm.** *J Comput Assist Tomogr* 2000;24:362–368